Available online at www.sciencedirect.com
SCIENCE DIRECT®
PERGAMON
International Journal of Heat and Mass Transfer 46 (2003) 2809–2818
International Journal of HEAT and MASS TRANSFER
www.elsevier.com/locate/ijhmt

Effect of the potential field on non-Fickian diffusion problems in a sphere

Han-Taw Chen [a,*], Kuo-Chi Liu [b]

[a] Department of Mechanical Engineering, National Cheng Kung University, Tainan 701, Taiwan, ROC
[b] Department of Mechanical Engineering, Far East College, Tainan 744, Taiwan, ROC

Received 8 September 2001; received in revised form 9 January 2003

Abstract

The present study applies a hybrid numerical method to investigate the effect of a potential field on one-dimensional non-Fickian diffusion problems in a sphere. This hybrid numerical scheme involves the Laplace transform technique and the control volume method in conjunction with the suitable hyperbolic shape functions. The Laplace transform method is used to remove the time-dependent terms in the governing differential equation and boundary conditions, and then the transformed equations are discretized by the control volume scheme. It is worth noting that the boundary condition at $r = 0$ should be carefully established for the present problems to determine an accurate numerical result. To evidence the accuracy of the present numerical method, a comparison of the mass concentration distribution between the present numerical results and the analytic solutions is made for the potential gradient $dV/dr = 0$. The results show that the present numerical results agree well with the analytic solutions and do not exhibit numerical oscillations in the vicinity of the jump discontinuity for various potential values. The important findings are that dV/dr has a great effect on the mass concentration distribution, and the strength of the jump discontinuity can decrease with increasing the value of the dimensionless potential gradient.

1. Introduction

Many studies for mass diffusion are conducted by using the traditional Fickian diffusion model. This model can give good approximations for most engineering applications [1–3]. The traditional Fickian diffusion equation belongs to the diffusion equation of the parabolic type. It is well known that the solution obtained from this traditional model exhibits an infinitely fast propagation of the mass signal. This concept can be unrealistic from a physical point of view. On the other hand, this traditional model may break down for the short-time inertial motion because the mass transport can have a phenomenon of the wave-like propagation [4–6]. Thus the non-Fickian diffusion equation (NFDE) that describes the mass diffusion with a finite speed of propagation is postulated. Das [5,6] has derived a NFDE in the presence of a potential field from the Kramers equation which describes the dynamics of a Brownian particle at a microscopic level. This equation can yield one physical quantity which retains the full short-time behavior, and is referred as the partial differential equation of the hyperbolic type. On the whole, the properties of the hyperbolic diffusion in heat transfer have received more attention than in mass transfer. Because the experimental techniques of studying short-time dynamics were innovated, the non-Fickian equation may be applied to the physical systems of practical interest, such as superionic conductors, molten salts, and neutron diffusion in nuclear reactors. The NFDE in the absence of potential field could be referred to as the hyperbolic heat conduction equation [7–13]. It can be found from our previous works [14,15] show that the potential field plays an important role in the non-Fickian diffusion problems.

Various numerical methods have been proposed for solving the hyperbolic heat conduction problems [7–12].

* Corresponding author. Fax: +886-6-235-2973.
E-mail address: htchen@mail.ncku.edu.tw (H.-T. Chen).

0017-9310/03/$ - see front matter
doi:10.1016/S0017-9310(03)00064-4

Nomenclature

C	dimensionless mass concentration, C^*/C_0	r	radial coordinate
C_0	reference mass concentration	s	Laplace transform parameter
C^*	mass concentration	T	temperature
$\widetilde{C}$	Laplace transform of C	t	time
D	diffusion coefficient, $k_B T\tau/m$	U	dependent variable, ηC
J^*	mass flux	V	potential field
J	dimensionless mass flux, $J^*/(C_0\sqrt{D/\tau})$	V_D	propagation speed of mass wave, $(D/\tau)^{1/2}$
k_B	Boltzmann constant		
ℓ	dimensionless distance between two neighboring nodes	*Greek symbols*	
		η	dimensionless space variable, $r/\sqrt{D\tau}$
m	particle mass	γ	friction parameter
P	dimensionless potential gradient, $(-\mathrm{d}V/\mathrm{d}r)/(m\sqrt{D/\tau^3})$	λ	parameter, $(s^2+s)^{1/2}$
		τ	relaxation time, $1/\gamma$
R	radius of a sphere	ξ	dimensionless time, t/τ

It can be observed from these previous works [7–12] that the major difficulty encountered in the numerical solution of the hyperbolic heat conduction problems is numerical oscillations in the vicinity of sharp discontinuities. Zhang and Liu [13] determined the analytical solution of the rapid transient heat conduction problem with non-Fourier effects in a solid sphere. Due to the existence of the potential field, the non-Fickian diffusion problems are more difficult to be solved than the hyperbolic heat conduction problems. Chen and Liu [14,15] have proposed a hybrid application of the Laplace transform technique and the control volume formulation in conjunction with the hyperbolic shape functions to solve the non-Fickian diffusion problems in the rectangular coordinate system. Because of the inherent nature of spherical problems, there exists a singular point at $r = 0$ in the present problems. Thus it is more difficult to be solved for the present problems than that in the rectangular coordinate system. The purposes of the present study are to develop a numerical method for the non-Fickian diffusion problems in the spherical coordinate system and are to investigate the effect of a potential field on the mass concentration distribution.

2. Mathematical formulation

The one-dimensional mass transfer in a sphere of radius R governed by the balance equation can be expressed as

$$\frac{\partial C^*}{\partial t} + \frac{\partial J^*}{\partial r} + \frac{2}{r} J^* = 0 \quad \text{in } 0 \leqslant r \leqslant R, \quad t > 0 \tag{1}$$

where J^* is the mass flux, C^* is the mass concentration, t is time, and r denotes the radial coordinate.

To accommodate the assumption of a local Maxwellian equilibrium, the generalized Fick's law from the Kramers equation can be written as [5,6]

$$J^* = -\frac{1}{\gamma}\frac{\partial J^*}{\partial t} - D\frac{\partial C^*}{\partial r} - \frac{\mathrm{d}V}{\mathrm{d}r}\frac{C^*}{m\gamma} \tag{2}$$

or

$$J^* = -\tau\frac{\partial J^*}{\partial t} - D\frac{\partial C^*}{\partial r} - \tau\frac{\mathrm{d}V}{\mathrm{d}r}\frac{C^*}{m} \tag{3}$$

where γ can be regarded as a friction parameter with the dimension of inverse time, m is the particle mass, $V(r)$ is the potential field, and $\tau = 1/\gamma$ is the relaxation time of the mass flux. $D = k_B T\tau/m$ is the diffusion coefficient and is assumed constant in the present study. T is the temperature. k_B is the Boltzmann constant.

For convenience of the numerical analysis, the following dimensionless parameters are introduced as

$$C = \frac{C^*}{C_0}, \quad \eta = \frac{r}{\sqrt{D\tau}}, \quad J = \frac{J^*}{C_0\sqrt{D/\tau}}, \quad \text{and} \quad \xi = t/\tau \tag{4}$$

where C_0 is the reference mass concentration. The short time domain $\xi \ll 1$ can be regarded as an interval in which the particle has not suffered many collisions and retains an inertial property. For the long time domain $\xi \gg 1$, the particle's dynamics loses its inertial property and becomes collision-dominated [6]. On the other hand, the NFDE describes a wave-like behavior at the short time $\xi \leqslant 1$ and a diffusive behavior at the long time $\xi > 1$.

Introducing these dimensionless variables in Eq. (4) into Eqs. (1) and (2) leads to the following dimensionless forms as

$$\frac{\partial C}{\partial \xi}+\frac{\partial J}{\partial \eta}+\frac{2}{\eta}J=0 \tag{5}$$

and

$$J=-\frac{\partial J}{\partial \xi}-\frac{\partial C}{\partial \eta}+PC \tag{6}$$

where $P=(1/(m\sqrt{D/\tau^3}))\left(-\frac{\mathrm{d}V}{\mathrm{d}r}\right)$ is defined as the dimensionless potential gradient. Das stated [6] that the term "$-\mathrm{d}V(r)/\mathrm{d}r$" can be regarded as a drift force. Thus the dimensionless potential gradient P can be regarded as the ratio between the drift force and the short-time inertial force.

Elimination of the dimensionless mass flux J from Eqs. (5) and (6) leads to a dimensionless description of NFDE with a potential field in a sphere as

$$\frac{\partial C}{\partial \xi}+\frac{\partial^2 C}{\partial \xi^2}=\frac{1}{\eta^2}\frac{\partial}{\partial \eta}\left(\eta^2\frac{\partial C}{\partial \eta}\right)-\frac{1}{\eta^2}\frac{\partial}{\partial \eta}(\eta^2 PC) \tag{7a}$$

or

$$\frac{\partial C}{\partial \xi}+\frac{\partial^2 C}{\partial \xi^2}=\frac{2}{\eta}\left(\frac{\partial C}{\partial \eta}-PC\right)-\frac{\partial}{\partial \eta}(PC)+\frac{\partial^2 C}{\partial \eta^2} \tag{7b}$$

It can be observed that a potential field term is included in Eq. (7a). If the inertial term $\partial^2 C/\partial \xi^2$ is neglected, Eq. (7a) will become the classical diffusion equation in the presence of a potential field. However, Eq. (7a) will become the type of the hyperbolic heat conduction equation provided that the potential field is absent, i.e. $P=0$. Thus the short-time behavior of the mass diffusion can be expected for such problems. Numerical solutions of Eq. (7a) for $P=0$ can be easily determined from the work of Lin and Chen [9]. To the best of the authors' knowledge, there is no report of such a study in the open literature and $(1/\eta^2)(\partial/\partial\eta)(\eta^2 PC)\neq 0$. The second term on the right-hand side of Eq. (7a) can be regarded as the drift term due to the existence of the potential field $V(r)$ [6].

Special consideration must be given to the central node at $\eta=0$ because this node is a singular point for the present problems. On the other hand, the first term on the right-hand side of Eq. (7b), $(2/\eta)(\partial C/\partial\eta-PC)$, at $\eta=0$ is indeterminate. However, the present problems subject to this condition that the mass concentration remains finite at $\eta=0$. Thus the boundary condition at $\eta=0$ should be given as

$$\frac{\partial C}{\partial \eta}-PC=0 \quad \text{at } \eta=0 \tag{8}$$

An interesting finding from Eqs. (6) and (8) is that the mass flux at $r=0$ can be regarded as zero.

In all examples of this paper, the initial conditions are given as

$$C(0,\eta)=0 \quad \text{and} \quad \frac{\partial C(0,\eta)}{\partial \xi}=0 \tag{9}$$

Various types of the boundary conditions will be discussed in the following examples.

3. Numerical analysis

To determine the present results easily, the transformation of the dependent variable is applied to transform the present problem into a problem in the rectangular coordinate system [16]. This new dependent variable $U(\eta,\xi)$ is defined as

$$U=\eta C \tag{10}$$

Due to the introduction of Eq. (10), Eq. (7a) can be rewritten as

$$\frac{\partial U}{\partial \xi}+\frac{\partial^2 U}{\partial^2 \xi}=\frac{\partial^2 U}{\partial \eta^2}-\frac{1}{\eta}\frac{\partial}{\partial \eta}(\eta PU) \tag{11}$$

It is obvious that the node at $\eta=0$ also is a singular point for Eq. (11). On the other hand, the second term on the right-hand side of Eq. (11), $(1/\eta)[\partial(\eta PU)/\partial\eta]$, at $\eta=0$ is indeterminate. However, the $U(\eta,\xi)$ value remains finite at $\eta=0$. Thus the boundary condition at $\eta=0$ for Eq. (11) should be given as

$$\frac{\partial}{\partial \eta}(\eta PU)=0 \quad \text{at } \eta=0 \tag{12}$$

But, the boundary condition at $\eta=0$ for Eq. (11) can be also obtained from the definition of $U(\eta,\xi)$ shown in Eq. (10) as

$$U(\eta,\xi)=0 \quad \text{at } \eta=0 \tag{13}$$

An interesting observation is that the boundary condition (13) coincides with Eqs. (8) and (12).

The Laplace transform technique is applied to remove the ξ-dependent terms in Eq. (11). The Laplace transform of Eq. (11) with respect to ξ is

$$\frac{\mathrm{d}^2\widetilde{U}}{\mathrm{d}\eta^2}-\lambda^2\widetilde{U}-\frac{1}{\eta}\frac{\mathrm{d}}{\mathrm{d}\eta}(\eta P\widetilde{U})=0 \tag{14}$$

where λ is defined as $\lambda=(s^2+s)^{1/2}$ for the NFDE and $\lambda=s^{1/2}$ for the Fickian diffusion equation (FDE). The Laplace transform parameter s is a complex variable. $\widetilde{U}$ is the Laplace transform of the dependent variable $U(\eta,\xi)$ and is defined as

$$\widetilde{U}(\eta,s)=\int_0^\infty \mathrm{e}^{-s\xi}U(\eta,\xi)\,\mathrm{d}\xi \tag{15}$$

Subsequently, Eq. (14) is discretized by using a control volume formulation. Integration of Eq. (14) within the ith control volume $[\eta_i-\ell/2,\eta_i+\ell/2]$ gives

$$\int_{\eta_i-\ell/2}^{\eta_i+\ell/2}\left[\frac{\mathrm{d}^2\widetilde{U}}{\mathrm{d}\eta^2}-\lambda^2\widetilde{U}-\frac{1}{\eta}\frac{\mathrm{d}}{\mathrm{d}\eta}(\eta P\widetilde{U})\right]\eta\,\mathrm{d}\eta=0 \tag{16}$$

where ℓ denotes the distance between two neighboring nodes and is uniform in the present study.

Before performing the integration of Eq. (16), $\widetilde{U}$ will be approximated by using the nodal values and the shape functions within the ith control volume $[\eta_i-\ell/2, \eta_i+\ell/2]$. The shape functions in the transform domain can be arbitrarily chosen for the parabolic diffusion problems. But they must be carefully chosen for the hyperbolic diffusion problems in order to determine a more accurate result. The works of Chen and Lin [8–10] and Chen Liu [14,15] showed that the selection of the shape functions in the control volume formulation is an important step for accurately determining the required results. Poor selection of the shape functions may produce severe numerical oscillations in the vicinity of jump discontinuities. The previous works [8–10,14,15] also showed that the hyperbolic shape functions derived from the associated homogeneous differential equation in the transform domain can be successfully applied to suppress numerical oscillations. Thus the shape functions for the present study are obtained from the following homogeneous differential equation.

$$\frac{\mathrm{d}^2\widetilde{U}}{\mathrm{d}\eta^2}-\lambda^2\widetilde{U}=0 \quad \text{for} \quad \eta_i\leqslant\eta\leqslant\eta_{i+1} \quad \text{and} \quad i=1,2,\ldots,n-1 \tag{17}$$

The following simple notations must be used:

$$\widetilde{U}(\eta_i)=\widetilde{U}_i \quad \text{and} \quad \widetilde{U}(\eta_{i+1})=\widetilde{U}_{i+1} \tag{18}$$

The analytical solution of Eq. (17) in the interval $[\eta_i,\eta_{i+1}]$ with the boundary condition (18) is

$$\widetilde{U}(\eta)=N_1(\eta_{i+1})\widetilde{U}_i+N_2(\eta_i)\widetilde{U}_{i+1} \tag{19}$$

where $N_1(z)$ and $N_2(z)$ are denoted as the hyperbolic shape functions and are given by

$$N_1(z)=\frac{\sinh[\lambda(z-\eta)]}{\sinh(\lambda\ell)} \quad \text{and} \quad N_2(z)=\frac{\sinh[\lambda(\eta-z)]}{\sinh(\lambda\ell)} \tag{20}$$

Similarly, the analytical solution of Eq. (17) in the interval $[\eta_{i-1},\eta_i]$ is

$$\widetilde{U}(\eta)=N_1(\eta_i)\widetilde{U}_{i-1}+N_2(\eta_{i-1})\widetilde{U}_i \tag{21}$$

Substituting the approximation for $\widetilde{U}$ shown in Eqs. (19) and (21) into Eq. (16) and then evaluating the resulting integral can produce the following discretized form as

$$B_{i-1}\widetilde{U}_{i-1}+B_i\widetilde{U}_i+B_{i+1}\widetilde{U}_{i+1}=0, \quad i=2,3,\ldots,n-1 \tag{22}$$

where the coefficients B_{i-1}, B_i, and B_{i+1} are given as

$$B_{i-1}=\eta_i+(\eta_i-\ell/2)P_{i-1/2}\frac{\sinh(\lambda\ell/2)}{\lambda} \tag{23a}$$

$$B_i=-2\eta_i\cosh(\lambda\ell)-[(\eta_i+\ell/2)P_{i+1/2}-(\eta_i-\ell/2)P_{i-1/2}]\frac{\sinh(\lambda\ell/2)}{\lambda} \tag{23b}$$

$$B_{i+1}=\eta_i-(\eta_i+\ell/2)P_{i+1/2}\frac{\sinh(\lambda\ell/2)}{\lambda} \tag{23c}$$

In Eqs. (23a) and (23b), $P_{i-1/2}$ and $P_{i+1/2}$ denote $P(\eta_i-\ell/2)$ and $P(\eta_i+\ell/2)$, respectively.

Rearrangements of Eq. (22) in conjunction with the discretized forms of the boundary conditions yield the following matrix equations as

$$[B][\widetilde{U}]=[F] \tag{24}$$

where $[B]$ is a band-matrix with the Laplace transform parameter s, $[\widetilde{U}]$ is a matrix representing the unknown nodal values in the transform domain, and $[F]$ is a matrix representing the forcing term. The application of the Gaussian elimination algorithm and the numerical inversion of the Laplace transform [17,18] to Eq. (24) can yield the value of U in the physical domain [19,20].

The value of U/η at $\eta=0$ in Eq. (10) is indeterminate and must be replaced by its limit as $\eta\to 0$ (or $r\to 0$). Thus the $C(0,\xi)$ value can be evaluated by using L'Hôspital's rule as

$$C(\eta,\xi)=\lim_{\eta\to 0}\frac{U}{\eta}=\frac{\mathrm{d}U}{\mathrm{d}\eta} \quad \text{at } \eta=0 \tag{25}$$

4. Results and discussion

To investigate the effect of a potential field on the mass concentration distribution of non-Fickian diffusion, various potential fields are illustrated. All the computations are performed with the uniform space size ($\ell=0.01$).

4.1. Example 1: Constant P and constant surface concentration

The first example considers a problem in solid a sphere of the dimensionless radius $\eta=1$ with the dimensionless boundary condition as

$$C(1,\xi)=1 \tag{26}$$

Thus the analytical solution of $C(\eta,\xi)$ for the solid sphere with $P=0$ can be determined as

$$C(\eta,\xi) = L^{-1}\left[\frac{\sinh(\lambda\eta)}{\eta\sinh(\lambda)s}\right] \tag{27}$$

Thus the $C(0,\xi)$ value for $P=0$ can be evaluated by using L'Hôspital's rule as

$$C(0,\xi) = \lim_{\eta\to 0} C(\eta,\xi) = L^{-1}\left[\frac{\lambda}{\sinh(\lambda)s}\right] \tag{28}$$

Zhang and Liu [13] has determined the analytical solution of $C(\eta,\xi)$ for $P=0$, as shown in Eq. (27). In order to show the accuracy of the present numerical method, the comparison of the dimensionless mass concentration distribution $C(\eta,\xi)$ between the present numerical results and the analytical solution for $P=0$ at various ξ values is shown in Fig. 1. It can be seen that the present numerical results agree well with the analytical solutions and do not exhibit severe numerical oscillations in the vicinity of the jump discontinuity. In general, the major difficulty in the numerical solution of the hyperbolic diffusion problem is numerical oscillations in the vicinity of the jump discontinuity [8–12].

Fig. 2(a) and 2(b) respectively show the distributions of the dimensionless mass concentration $C(\eta,\xi)$ at $\xi=0.9$ for various P values. It can be seen that the present numerical results do not exhibit severe oscillations in the neighborhood of the jump discontinuity for various P values. This implies that the present numerical scheme can successfully suppress these numerical oscillations. On the other hand, the present numerical method should have good accuracy for such problems.

It can be observed from Figs. 1 and 2 that the location of the jump discontinuity at a specific dimensionless time is the same for various P values. These results show

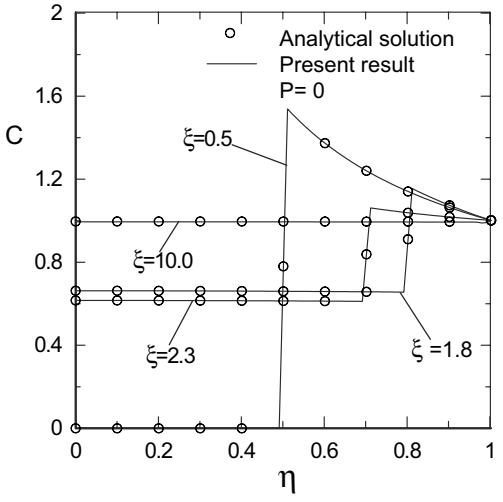

Fig. 1. Comparison of $C(\eta,\xi)$ between the analytical solutions and present results at various ξ values for $P=0$.

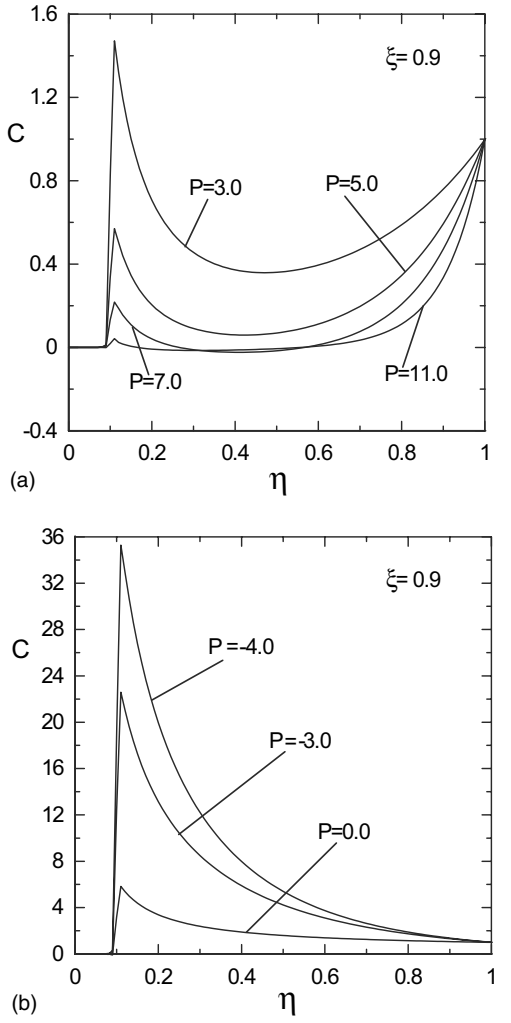

Fig. 2. Profiles of $C(\eta,0.9)$ for $C(1,\xi)=1.0$ and various P values: (a) $P>0$ and (b) $P\leqslant 0$.

that the mass wave propagates in a similar manner for the rectangular and spherical coordinate systems [9]. This phenomenon can be explained from the definition of the propagation speed of the mass wave V_D that can be defined as $V_D=(D/\tau)^{1/2}$. This implies that the propagation speed is independent of the geometry and the potential gradient and depends only on the mass diffusivity D and the relaxation time τ. Thus the position of the mass wave front is the depth of the mass wave penetrating into the substance and is equal to tV_D. The mass wave induced by the boundary condition at $\eta=1$ has not yet reached the center at $\xi<1.0$ for various $P(\eta)$ values. Under this circumstance, this case can be regarded as a semi-infinite problem. This implies that the boundary condition at $\eta=0$ can be written as $C(0,\xi)=0$ and $\partial C(0,\xi)/\partial\eta=0$ at $\xi<1.0$. It is found

that these conditions also satisfy the boundary condition shown in Eq. (8).

It can be observed from Fig. 2 that the effect of $P(\eta)$ on the dimensionless mass concentration $C(\eta,\xi)$ is very great at a specific ξ value and the strength of the jump discontinuity reduces with increasing the P value. On the other hand, this strength of the jump discontinuity or the peak value of the mass concentration seems to increase with decreasing the P value. The similar phenomena can be found from our previous works [14,15]. In accordance with the definition of $P(\eta)$, the above result implies that the potential gradient $\mathrm{d}V/\mathrm{d}r$ or the curve of $V(r)$ has a great effect on the mass concentration distribution. Another feature of a NFDE is that the solution of the mass concentration be generally non-negative. However, it can be found that $C(\eta,\xi)$ at $\xi = 0.9$ can exhibit the non-positive values for $P < 7.0$.

Fig. 3 shows the history of the dimensionless mass concentration $C(\eta,\xi)$ at $\eta = 0.7$ for $P(\eta) = -2.0$ and 2.0. This figure exhibits the wave-like behavior. However, this wavy behavior obviously dissipates with time.

Fig. 4(a) and (b) show the profiles of $C(\eta,\xi)$ at various ξ values for $P(\eta) = -2.0$ and 2.0. It can be seen that there exists no numerical oscillation in the vicinity of the jump discontinuity. At the same time, Figs. 1 and 4 also show that, at $\xi = 0.5$, the mass wave induced by the outer boundary condition only reaches the location $\eta = 0.5$ and has not yet reached the center for $P(\eta) = -2$, 0, and 2. On the other hand, the region, $0.0 \leqslant \eta < 0.5$, is not yet affected by the boundary condition at $\eta = 1$. Afterward, the reflected mass wave interacts with the original mass wave at $\xi = 1.8$ and 2.3. It is interesting that a superposition of the reflected and original waves results in the occurrence of the peak value

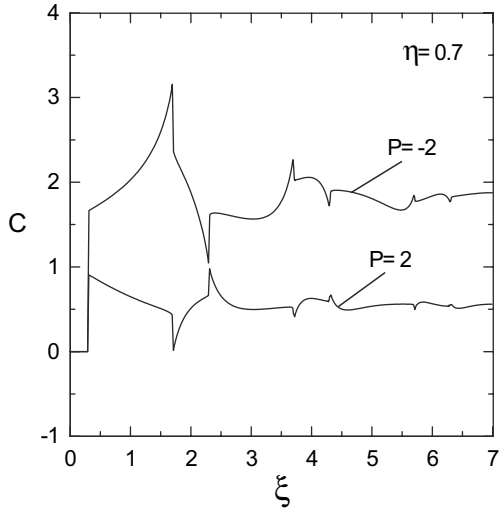

Fig. 3. History of $C(0.7,\xi)$ for $C(1,\xi) = 1.0$ with respect to $P(\eta) = -2.0$ and 2.0.

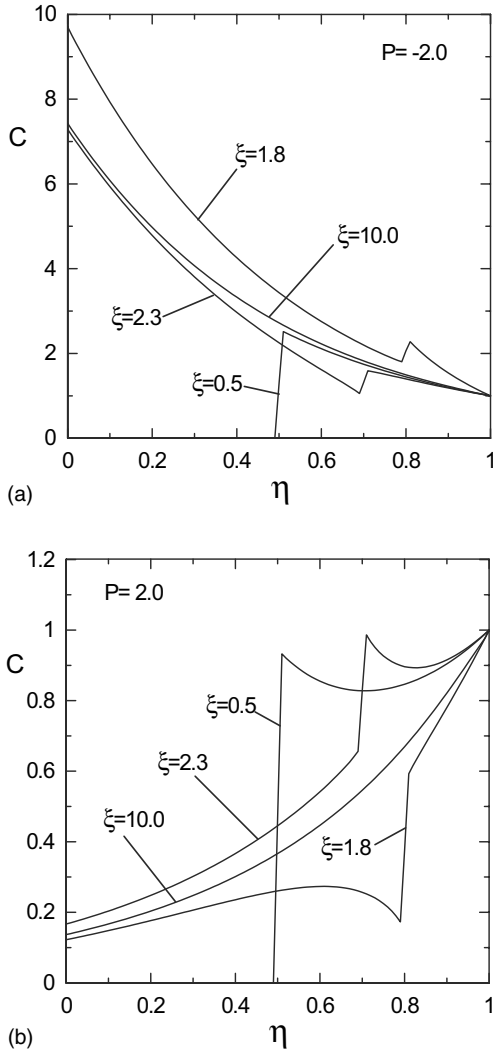

Fig. 4. Profiles of $C(\eta,\xi)$ at various ξ values for $C(1,\xi) = 1.0$: (a) $P(\eta) = -2.0$ and (b) $P(\eta) = 2.0$.

in the middle region of the domain at $\xi = 1.8$ and 2.3. However, the profile of $C(\eta,\xi)$ at $\xi = 10$ does not reveal the phenomenon of the jump discontinuity and is the same as that obtained from the FDE. This implies that the non-Fickian effects are significant only for very short times and dissipate with time. The foregoing results show that the profiles of $C(\eta,\xi)$ for the non-Fickian diffusion problems reveal a wave-like behavior at the short time $\xi \leqslant 1$ and a diffusive behavior at the long time $\xi > 1$. This also implies that the non-Fickian effects are significant only for very short times and dissipate with time. Though these are physically doubtful results, they are admitted for the wave propagation concept. These doubtful solutions can be only evidenced through further experiments whether they are accurate or not.

4.2. Example 2: Constant P and time-dependent surface concentration

This illustrative problem concerns one case of practical interest that the surface concentration at $\eta = 1$ varies exponentially with the dimensionless time and approaches an equilibrium concentration. Obviously, the surface concentration is changed rapidly but not instantaneously. The dimensionless boundary condition at $\eta = 1$ can be written as

$$C(1,\xi) = 1 - \exp(-\xi) \tag{29}$$

Fig. 5(a) and (b) show a comparison of the dimensionless mass concentration $C(\eta,\xi)$ between the hyperbolic model and the parabolic model at various ξ values for $P = -2$ and 2, respectively. It can be found that the difference between them is great for short time. This difference can result from the non-Fickian effect. An interesting observation is that the value of $C(\eta,\xi)$ for the parabolic model is greater than that for the hyperbolic model at $\xi = 0.5$. However, the value of $C(\eta,\xi)$ for the parabolic model is less than that for the hyperbolic model at $\xi = 1.8$. These results also show that the non-Fickian effect is significant only for short time and quickly dissipates with time. An interesting observation is that the profile of $C(\eta,\xi)$ at $\xi = 1.8$ is nearly smooth for $P = -2$. However, there exists a discontinuous point for $P = 2$.

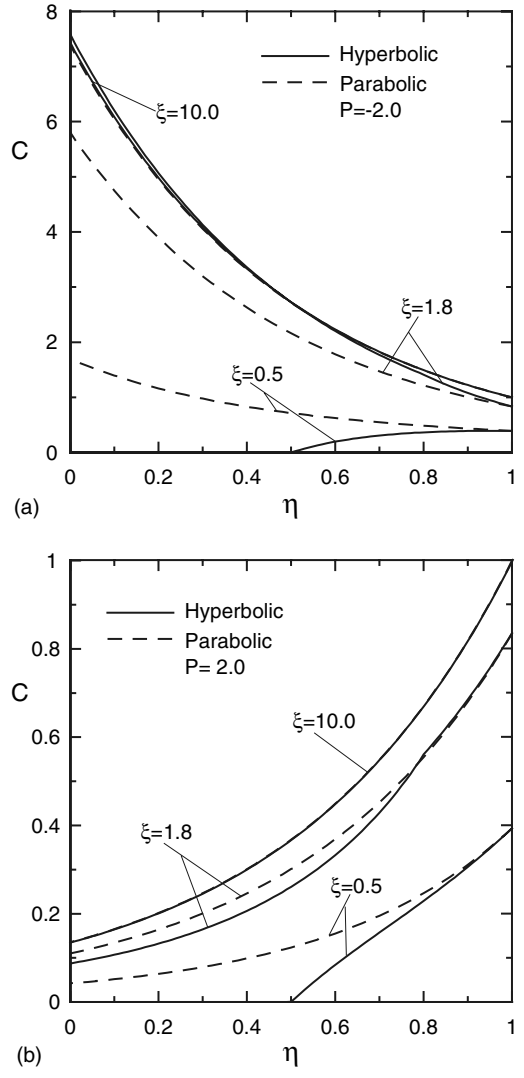

Fig. 5. Comparison of $C(\eta,\xi)$ between the hyperbolic model and parabolic model at various ξ values for $C(1,\xi) = 1 - \exp(-\xi)$: (a) $P = -2.0$ and (b) $P = 2.0$.

Fig. 6 shows a comparison between the hyperbolic model and the parabolic model at $\xi = 0.9$ for various P value. The deviation of $C(\eta,\xi)$ between the hyperbolic model and parabolic model is great for $P \leqslant 0$ and decreases with increasing the P value. An interesting observation is that the jump discontinuity in the previous figures disappears for the present case. This implies that the jump discontinuity in the solution of NFDE can be suppressed by the boundary condition with the feature of the rapid variation. However, the location of the mass wave front is still equal to tV_D and is independent of the potential gradient and the types of boundary conditions.

4.3. Example 3: Non-constant $P(\eta)$

The last example investigates the effect of the slowly and rapidly varying $P(\eta)$ on the dimensionless mass concentration $C(\eta,\xi)$ calculated from the NFDE. Two

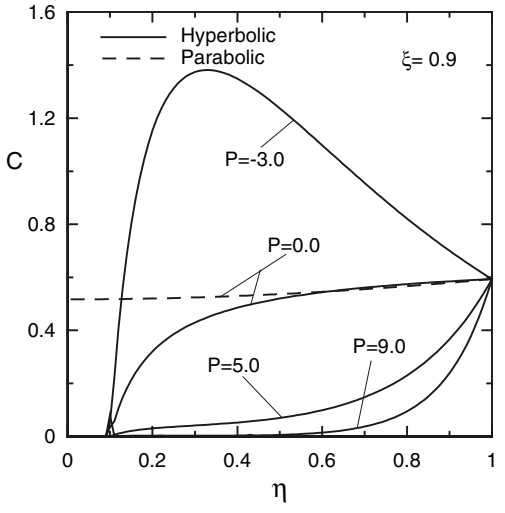

Fig. 6. Comparison of $C(\eta,0.9)$ between the hyperbolic model and parabolic model for various P values and $C(1,\xi) = 1 - \exp(-\xi)$.

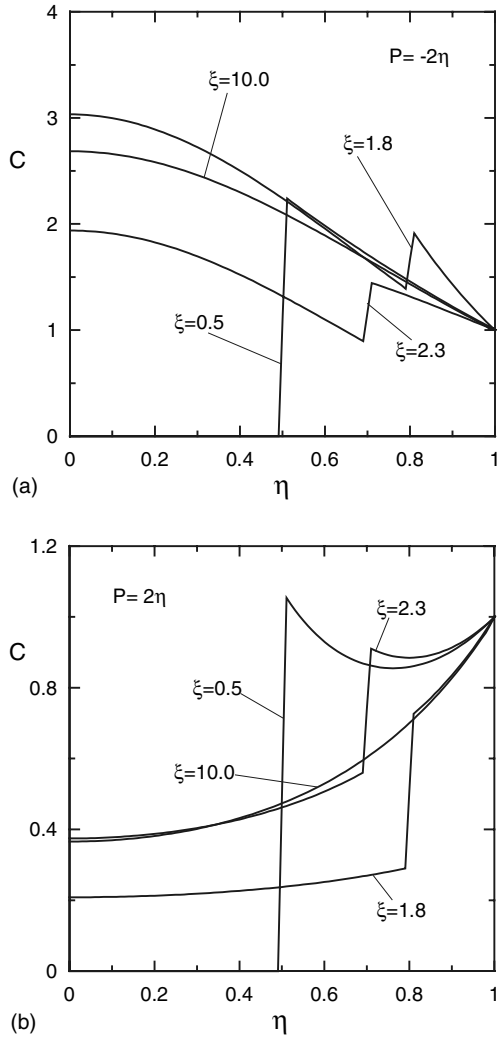

Fig. 7. Profiles of $C(\eta,\xi)$ at various ξ values for $C(1,\xi)=1.0$: (a) $P(\eta)=-2\eta$ and (b) $P(\eta)=2\eta$.

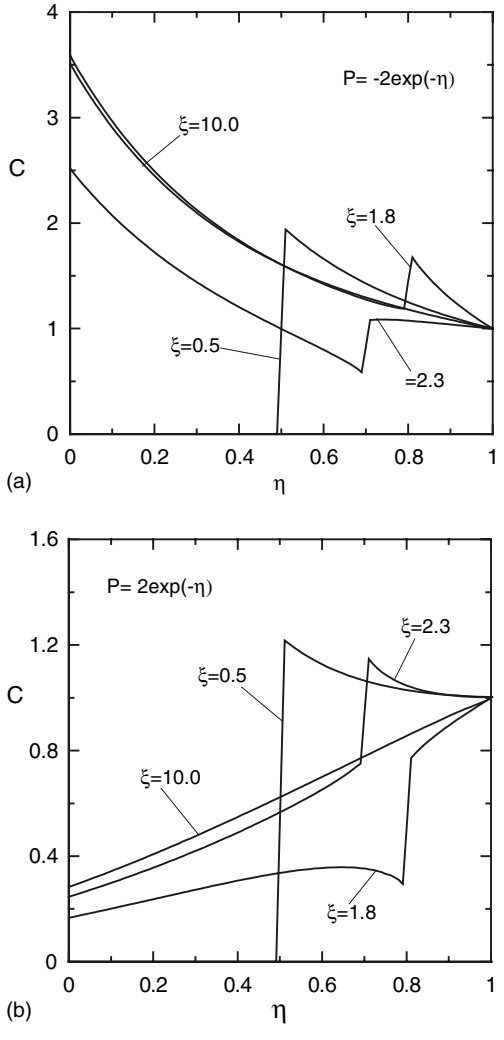

Fig. 8. Profiles of $C(\eta,\xi)$ at various ξ values for $C(1,\xi)=1.0$: (a) $P(\eta)=-2\exp(-\eta)$ and (b) $P(\eta)=2\exp(-\eta)$.

different functional forms of $P(\eta)$, such as $P(\eta)=\pm 2\eta$ and $P(\eta)=\pm 2\exp(-\eta)$, will be illustrated. The boundary conditions (26) and (29) are respectively applied to determine the numerical results shown in Figs. 7–10.

Figs. 7 and 8 respectively show the profiles of $C(\eta,\xi)$ at various ξ values for the boundary condition $C(1,\xi)=1$, as shown in Eq. (26), corresponding to $P(\eta)=\pm 2\eta$ and $P(\eta)=\pm 2\exp(-\eta)$. Similarly, it can be observed from Figs. 3, 7 and 8 that the location of the jump discontinuity at $\xi=0.5$ for a non-constant $P(\eta)$ is the same as that for a constant $P(\eta)$. This result further shows that the position of the mass wave front is independent of the functional form of the potential gradient. In other words, the propagation speed of the mass wave depends only on D and τ. As shown in Figs. 3, 7 and 8, the deviation of $C(\eta,\xi)$ between a constant $P(\eta)$ and non-constant $P(\eta)$, such as $P(\eta)=\pm 2\eta$ and $P(\eta)=\pm 2\exp(-\eta)$, is very great at various ξ values. These figures indicate that the rapidly varying $P(\eta)$ has a significant effect on the profile of $C(\eta,\xi)$ for various ξ values. These results evidence that the NFDE is very sensitive to the functional form of the dimensionless potential gradient $P(\eta)$. The similar result can be also found from Refs. [14,15].

The wave behavior shown in Figs. 7 and 8 is similar to that shown in Example 1 for the constant $P(\eta)$ under the same boundary conditions. The mass wave reaches the reflecting boundary surface at $\xi=1$. Afterward, the reflected mass wave interacts with the original mass wave at $\xi=1.8$ and 2.3. Due to a superposition of the reflected and original mass waves, the peak value of the mass concentration occurs in the middle region of

the domain at $\xi = 1.8$ and 2.3. The profile of $C(\eta, \xi)$ at $\xi = 10$ is essentially the same as that obtained from the FDE. Similarly, these results also imply that the non-Fickian effects will dissipate with time.

Figs. 9 and 10 show the profiles of the dimensionless concentration distributions $C(\eta, \xi)$ at various ξ values for the boundary condition $C(1, \xi) = 1 - \exp(-\xi)$, as shown in Eq. (29), corresponding to $P(\eta) = 2\eta$ and $2\exp(-\eta)$. As shown in Figs. 3, 7 and 8, the deviation of $C(\eta, \xi)$ between a constant $P(\eta)$ and non-constant $P(\eta)$, such as $P(\eta) = \pm 2\eta$ and $P(\eta) = \pm 2\exp(-\eta)$, is very great at various ξ values. An interesting observation from these two figures is that there exists the discontinuous point for the profile of $C(\eta, \xi)$ at $\xi = 1.8$ and 2.3. In addition, Figs. 5, 9, and 10 also show that the functional form of $P(\eta)$ has a significant effect on the profile of $C(\eta, \xi)$.

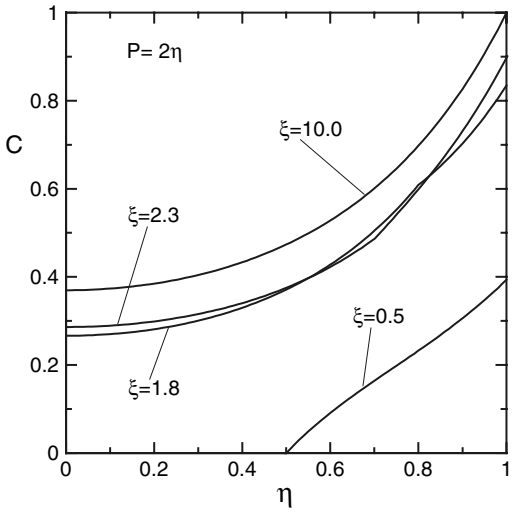

Fig. 9. Profiles of $C(\eta, \xi)$ at various ξ values for $C(1, \xi) = 1 - \exp(-\xi)$ and $P(\eta) = 2\eta$.

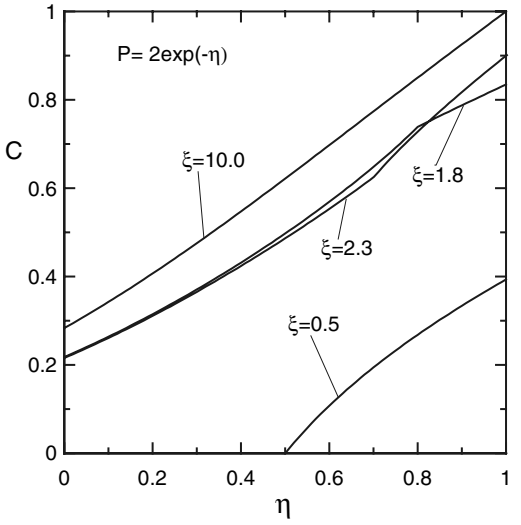

Fig. 10. Profiles of $C(\eta, \xi)$ at various ξ values for $C(1, \xi) = 1 - \exp(-\xi)$ and $P(\eta) = 2\exp(-\eta)$.

5. Conclusion

The present study applies a hybrid numerical method involving the Laplace transform technique and the control-volume method in conjunction with the hyperbolic shape functions to investigate the non-Fickian diffusion problems in the presence of a potential field in a solid sphere. Various illustrated examples show that the present numerical method can accurately determine the profile of the dimensionless mass concentration without any numerical oscillation around the jump discontinuity for various functional forms of the dimensionless potential gradient $P(\eta)$. The present results show that the non-Fickian effect is significant only for short time and quickly dissipates with time. The phenomenon of the jump discontinuity can be suppressed by the boundary condition. The speed of propagation of mass signal is independent of the functional form of $P(\eta)$ and the types of boundary conditions. An important result is that the rapidly varying $P(\eta)$ has a significant effect on the profile of $C(\eta, \xi)$ corresponding to various ξ values.

Acknowledgement

The authors wish to thank Prof. A.K. Das for giving us his valuable works.

References

[1] J. Crank, The Mathematics of Diffusion, second ed., Oxford University, New York, 1975.
[2] P. Shewmon, Diffusion in Solids, the Minerals, second ed., Metals and Materials Society, Pennsylvania, 1989 (Chapter 1).
[3] S. Ding, W.T. Petuskey, Solution to Fick's second law of diffusion with a sinusoidal excitation, Solid State Ionics 109 (1998) 101–110.
[4] S. Godoy, L.S. Garcia-Colin, From the quantum random walk to classical mesoscopic diffusion in crystalline solids, Phys. Rev. E 53 (1996) 5779–5785.
[5] A.K. Das, A non-Fickian diffusion equation, J. Appl. Phys. 70 (3) (1991) 1355–1358.
[6] A.K. Das, Some non-Fickian diffusion equation: theory and applications, Defect Diffus. Forum 162–163 (1998) 97–118.

[7] J.P. Wu, Y.P. Shu, H.S. Chu, Transient heat transfer phenomenon of two-dimensional hyperbolic heat conduction problem, Numer. Heat Transfer—Part A 33 (1998) 635–652.
[8] H.T. Chen, J.Y. Lin, Numerical analysis for hyperbolic heat conduction, Int. J. Heat Mass Transfer 36 (1993) 2891–2898.
[9] J.Y. Lin, H.T. Chen, Numerical solution of hyperbolic heat conduction in cylindrical and spherical systems, Appl. Math. Modell. 18 (1994) 384–390.
[10] H.T. Chen, J.Y. Lin, Analysis of two-dimensional hyperbolic heat conduction problems, Int. J. Heat Mass Transfer 37 (1994) 153–164.
[11] G.F. Carey, M. Tsai, Hyperbolic heat transfer with reflection, Numer. Heat Transfer 5 (1982) 309–327.
[12] D.E. Glass, M.N. Özisik, D.S. McRae, B. Vick, On the numerical solution of hyperbolic heat conduction, Numer. Heat Transfer 8 (1985) 497–504.
[13] Z. Zhang, D.Y. Liu, Non-Fourier effects in rapid transient heat conduction in a spherical medium, J. Eng. Thermophy. 19 (1998) 601–605.
[14] H.T. Chen, K.C. Liu, Numerical analysis of non-Fickian problems in a potential field, Numer. Heat Transfer—Part B 40 (2001) 265–282.
[15] H.T. Chen, K.C. Liu, Analysis of non-Fickian diffusion problems in a composite medium, Comp. Phy. Comm. 150 (2003) 31–42.
[16] M.N. Özisik, Heat Conduction, second ed., Oxford University, New York, 1980.
[17] G. Honig, U. Hirdes, A method for the numerical inversion of Laplace transforms, J. Comp. Appl. Math. 10 (1984) 113–132.
[18] W.M. Dubner, J. Abate, Numerical inversion of Laplace transforms by relating them to the finite Fourier cosine transform, J. ACM. 15 (1968) 115–123.
[19] H.T. Chen, T.M. Chen, C.K. Chen, Hybrid Laplace transform/finite element method for one-dimensional transient heat conduction problems, Comput. Meth. Appl. Mech. Eng. 63 (1987) 83–95.
[20] H.T. Chen, Hybrid method for transient response of circular pins, Int. J. Numer. Meth. Eng. 29 (1990) 303–314.